Since January 2020 Elsevier has created a COVID-19 resource centre with free information in English and Mandarin on the novel coronavirus COVID-19. The COVID-19 resource centre is hosted on Elsevier Connect, the company's public news and information website.

VIROLOGY 54, 37–52 (1973)

Aspects of the Developmental Morphology of California Encephalitis Virus in Cultured Vertebrate and Arthropod Cells and in Mouse Brain

MICHAEL J. LYONS AND JAROSLAV HEYDUK

Department of Microbiology, Cornell University Medical College, 1300 York Avenue, New York New York 10021

Accepted March 5, 1973

An electron microscopic study was made of the replication of California encephalitis (La Crosse strain) in cultured vertebrate cells (Vero, African green monkey kidney), in a line of cultured mosquito cells (*Aedes albopictus*), and in brain tissue of suckling mice. Morphologically similar virus particles, approximately 95 nm in diameter, were encountered in all three systems, and a common mode of virus assembly and maturation appeared to obtain. Virus assembly was shown to occur exclusively at internal cytomembrane interfaces, the Golgi complex appearing as the initial assembly site, which site became less focal as infection progressed due to the proliferation of Golgi smooth membranes and the dilation of cisternae and vesicles. The assembly process involved viral budding into cisternal and vesicular lumina, the virion thereby acquiring its limiting membrane. The envelope of such intracellular virions exhibited a poorly defined fringe, approximately 8 nm in width, which appeared to undergo a maturational change as the virions were discharged from the cell, such that, extracellularly, virions displayed a well-developed fringe, approximately 12 nm wide—a change especially noteworthy in the case of virions in infected mouse brain.

The presence was noted in infected Vero cells—and in one instance in an infected mosquito cell—of crescent-shaped segments of thickened cisternal membrane, which possibly represented an early phase of viral assembly in which nucleocapsid aligned itself in close apposition to a membrane segment preparatory to the initiation of budding.

In areas of the cytoplasm adjacent to sites of viral assembly in neurons, a fine granulofibrillar matrix was frequently found, enmeshed in which were numbers of 50–60 nm spherical structures. In a low proportion of cells from infected mosquito cultures, dense granulofibrillar masses were found in the cytoplasm.

In Vero cells, infection with CE virus was cytolytic, while in *A. albopictus* cells, no gross cytopathic effects were manifest, and persistently infected cultures developed upon subcultivation. However, less than 10% of challenged mosquito cells became productively infected and for a proportion of these, at least as determined by electron microscopy, the infection was lethal.

INTRODUCTION

The California encephalitis group of arboviruses includes important agents of human central nervous system disease, yet comparatively little is known about the fundamental biological, structural, and biochemical properties of the group. An original electron microscopic study of California encephalitis (CE) virus by Murphy and colleagues (1968a) revealed many unusual features of virus developmental morphology, notably, the comparatively large size of the virions (98 nm in average diameter, as compared to 55 nm and 38 nm for groups A and B arboviruses, respectively), their relatively unstructured interiors, and

their seeming exclusive assembly at internal cytomembrane interfaces. Later, the Bunyamwera viruses were shown to possess essentially similar features (Murphy *et al.*, 1968b), and in a recent preliminary survey, Holmes (1971) concluded that it was likely that members of the Bunyamwera Supergroup as a whole (W.H.O. Scientific Group on Arboviruses, *WHO Tech. Rep. Ser.* **396,** 1–32, 1967) and certain antigenically unrelated viruses such as Anopheles A, possessed common properties of size, structure, and mode of development comparable to those originally described for California encephalitis virus.

In the present investigation, representing part of a more general study of the ultrastructure and biochemical interactions of the large lipid-containing arboviruses, it was decided to employ CE virus as a model, to consolidate and further extend existing knowledge of the morphology of virus development. An electron microscopic study was made of virus replication in a continuous vertebrate (Vero) and an ecologically relevant invertebrate (*A. albopictus*) cell line. Information was sought on whether host-dependent nuances of difference obtained in these phylogenetically diverse systems. The utility of the suckling mouse brain system in the study of the morphology of virus replication had been amply demonstrated by Murphy *et al.* (1968a, b), in terms of high potential sensitivity to virus infection and high virus yields. In the present study, this *in vivo* system was studied in parallel with the *in vitro* systems, in the expectation that a more complete picture of events might be obtained.

MATERIALS AND METHODS

The virus. The La Crosse strain of CE virus was kindly provided by Dr. N. Karabatsos of the Yale Arbovirus Research Unit. This had been passaged 5 times intracerebrally in suckling mice, and for experiments covered in the present report, seed virus derived from 3 additional passages was used. This was in the form of 10% clarified mouse brain suspensions in Hanks' salts plus 1% bovine serum alumen. Titers ranged from 4.5 to 7.5 $\times$ 10^7 PFU/ml.

Experimental animals. One- to 2-day-old litters of Swiss albino mice were infected by the intracerebral inoculation of 0.02 ml of a 10-fold dilution of stock virus. Mice were sacrificed and samples of brain tissue taken for electron microscopy at stages from the first appearance of paralysis through to the moribund state, events which occurred on average from 38 to 46 hr post infection.

Cell cultures. Cells of the stable African green monkey kidney cell line (Vero) were obtained from the American Type Culture Collection (CCL-81). Growth medium consisted of Eagle's MEM (Hanks' salts) plus 7.5% newborn calf serum. MEM (Earle's salts) plus 2% serum was employed as maintenance medium.

Cells of the continuous mosquito cell line of *A. albopictus* (Singh, 1967) derived from insect larvae, were kindly provided by Dr. Arthur Greene, Institute of Medical Research, Camden, New Jersey. They were cultured in glass prescription bottles using a growth medium formulated by Dr. W. F. Scherer (personal communication) and consisting of 0.65% lactalbumen hydrolyzate, 0.5% yeast extract, *d*-glucose 0.4%, heat-inactivated newborn calf serum 5%, 1% of a 1.4% sodium bicarbonate solution, all in Hanks' BSS. Cells were cultivated at 30°C. For maintenance, the serum content was reduced to 2%.

Assay of infectious virus. A plaque assay based on the procedure of Stim and Henderson (1969) using Vero cell monolayer cultures was employed. Confluent cultures in 2-oz prescription bottles were washed with PBS and inoculated with virus diluted with 1% bovine serum albumen in Hanks' salts at pH 7.8. After absorption of 1.5 hr the virus inoculum was removed and an agar overlay medium was added. The overlay medium of Stim and Henderson (1969) was supplemented with lactalbumen hydrolyzate and yeast extract to concentrations of 0.18% and 0.05%. In addition, pancreatin (Came *et al.*, 1969) was added to a concentration of 0.33%. The agar concentration in the overlay was 0.9%. A second agar overlay containing Neutral Red indicator was added following an interval of 2 days. Plaques were read from 3 to 5 days after infection.

Growth curves. Cells were infected at a multiplicity of 10 PFU/cell. Following a 1.5-hr absorption period, the virus inoculum was removed, the cells were washed three times with PBS, and maintenance medium was added. The mosquito cells were maintained at 30°, the Vero cells at 37°. Samples were withdrawn at intervals following infection and stored at −70° for subsequent assay. For estimation of cell-associated virus, cell sheets were washed with PBS, resuspended in Hanks' BA medium, sonicated, and clarified by low speed centrifugation. Such cell-derived supernatants were stored and assayed as indicated above.

Infectious center assay. Infected mosquito cells were trypsinized, dispersed and washed in growth medium, and incubated for 15 min at room temperature in a heat-inactivated hyperimmune serum prepared in guinea pigs, diluted 1:10. After two further washes in growth medium, counting in a hemacytometer, and appropriate dilution in medium, one cell in 0.1 ml was seeded into each of 96 wells (0.4 ml capacity) of a plastic tray (Model 15-FB-96-TC, Limbro Chemical Co., Inc.). Two trays were used per assay. Trays were sealed and returned to the 30° incubator. After overnight incubation each well was seeded with 25,000 Vero cells in 0.2 ml of Vero maintenance medium, and trays were resealed and returned to the 37° incubator. Vero cell monolayers were rapidly established and observed over several days for the development of cytopathic effects. The infectious center assay of Vero cells was similarly conducted.

Electron microscopy. Immediately after sacrifice, the brains of suckling mice were excised and randomly cut into 1 mm^3 blocks in ice-cold 2.5% phosphate-buffered glutaraldehyde at pH 7.2. After fixation for 1 hr at 4°, and removal of excess glutaraldehyde by washing, specimens were postfixed for 1 hr at 4° in 1% phosphate-buffered osmium tetroxide. After a series of dehydration steps in graded aqueous ethanol solutions, specimens were embedded in Epon. Sections were cut with a Porter-Blum MT-2 ultramicrotome equipped with glass knives, then stained for 20 min with 4% sq. uranyl acetate followed by 10 min in an 0.5% alkaline lead citrate stain. For electron microscopy, an AEI-6B electron microscope was used, operating at 60 kV, using an objective aperture of 50 μm, and instrumental magnifications of × 7,500–30,000.

Cell monolayers were usually prefixed *in situ* with the glutaraldehyde fixative for 1 hr, then were rinsed and suspended in phosphate buffer and pelleted by centrifugation for 15 min at 6000 rpm at 4°C. The pellets were removed, sliced into 1 mm^3 blocks in osmium tetroxide, postfixed, and processed as above.

RESULTS

Growth Kinetics of California Encephalitis virus in Vero and A. albopictus Cell Cultures

CE virus appeared to be less efficiently adsorbed to mosquito cells than to Vero cells; between 70 and 75% of input virus was elutable from the former cells at the end of a 1.5-hr adsorption period whereas the corresponding figure for Vero cells was approximately 20%. However, virus growth curves in the mosquito cells at adsorbed input multiplicities in the range 2–10 PFU/cell were indistinguishable. Figure 1 depicts comparative growth curves of CE virus in Vero and *A. albopictus* cells. After an eclipse phase lasting 4–6 hr, virus replicated exponentially, reaching maximal titers 20–24 hr post infection. The yields of cell-associated virus closely paralleled released virus, indicating a rapid release of virus from infected cells. In the mosquito cell cultures, the ratio of released to cell-associated virus, 24 hours post infection was 5.8:1, whereas in Vero cultures this ratio approximated unity.

The results of an infectious center assay are presented in Table 1. The percentage of infected mosquito cells (9.4) was significantly less than that of infected Vero cells (81.0%). It was calculated that the yield of virus per infected mosquito cell was approximately 40 PFU/cell, somewhat higher than a corresponding figure 25 PFU per infected Vero cell.

The outcome of infection in Vero cells was cell lysis. Cytopathic effects, involving increasing cytoplasmic granularity, pycnosis, cytoplasmic retraction, cell rounding, and

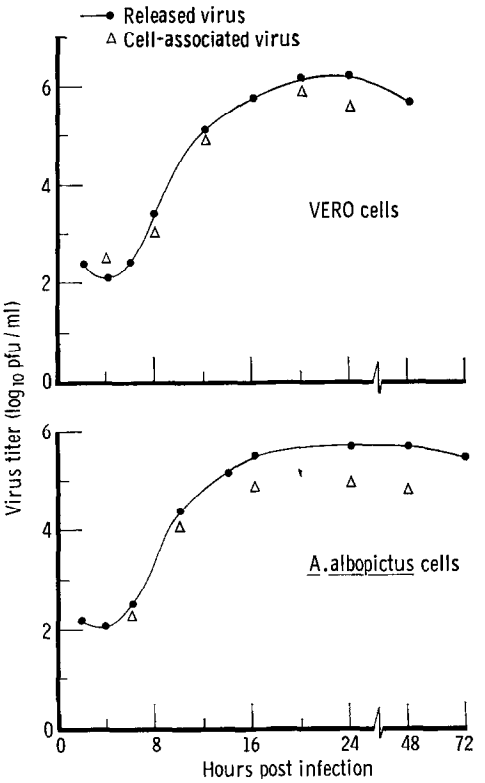

FIG. 1. Growth curve of California encephalitis virus in Vero cells (top) and in *A. albopictus* cells (bottom) following infection of confluent monolayers of cells at a multiplicity of 10 PFU/cell. Titers of virus released into the medium and cell-associated virus were assayed by the plaque method as described under Materials and Methods.

eventual detachment from the surface of the culture bottles, first detectable in a small percentage of the cells 24 hr p.i., progressively involved the majority of cells by 48–72 hr p.i. This CE virus–Vero cell interaction contrasted sharply with observations in the infected mosquito cultures. Here, the infection was seemingly moderate, no gross cytopathic effects were apparent, and cultures could be maintained with replenishment of medium for at least 2 weeks without subcultivation. As indicated in Table 2, such infected cultures could be serially subcultivated yielding cultures which remained persistently infected.

The replication of virus in suckling mouse brain cells was similar to that recorded by

TABLE 1

INFECTIOUS CENTER ASSAY: PERCENTAGE OF INFECTED *A. albopictus* CELLS AND VERO CELLS 20 HOURS AFTER INFECTION WITH CALIFORNIA ENCEPHALITIS VIRUS (m.o.i. = 10 PFU/cell)

Cells	No. of cells plated	No. of wells showing lysis	% infected cells
A. albopictus	192	18	9.4
Vero	192	156	81.0

TABLE 2

TITERS OF CE VIRUS IN FLUID HARVESTS OF SERIALLY PASSAGED INFECTED *A. albopictus* CELLS[a]

Passage level	Titer (PFU/ml)
1	2.7×10^5
2	1.8×10^4
6	8.6×10^4
10	4.1×10^4
13	3.0×10^4
14	9.1×10^4

[a] Confluent cultures subcultivated at splitting ratio of 1:6 at weekly intervals.

Murphy *et al.* (1968a), maximal titers being reached 34–40 hr after infection.

Electron Microscopy of Infected Vero Cells

With specimens harvested before 16 hours post infection, electron microscopy was generally unrewarding. However, at later times, as intra- and extracellular titers reached a maximum, evidence of virus replication was found in a majority of cells and virus was readily observed extracellularly. The Golgi complex appeared to be the cellular site at which virus replication was initiated. As a consequence of infection, a marked dilation of Golgi cisternae and vesicles occurred, concomitant with the proliferation of sheets and tubular elements of smooth unit membranes, presenting numerous sites for virus assembly. Representative of such a situation are the fields depicted in Fig. 2 and 3, from specimens sampled 20 and 36 hr after infection, respectively. In Fig. 2, facets of the viral assembly process are represented. Virus particles ap-

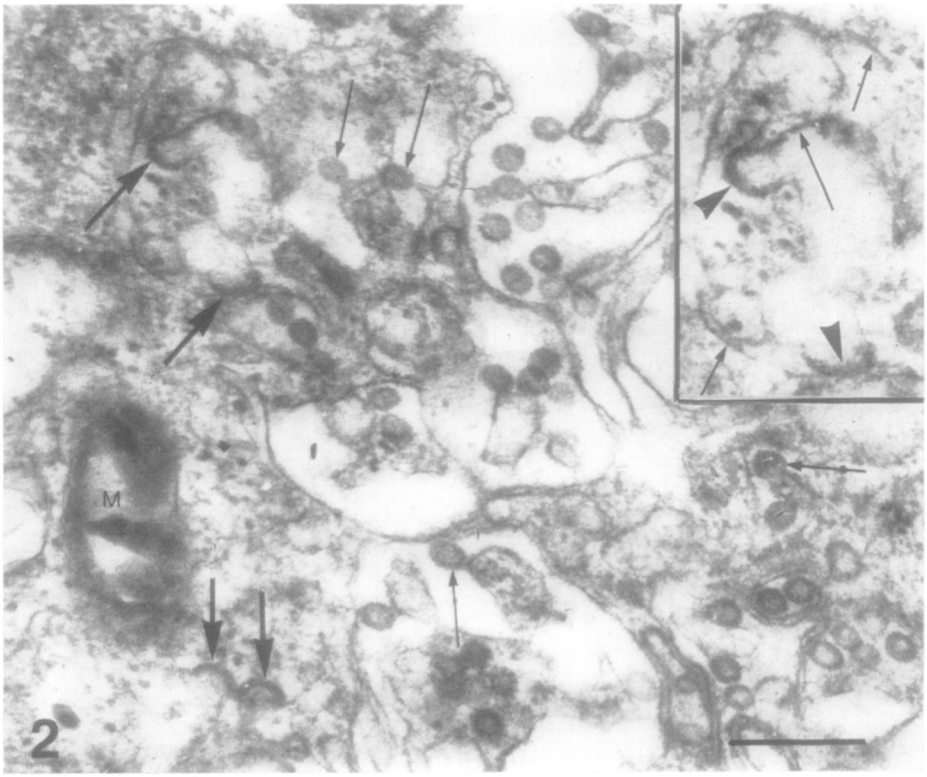

FIG. 2. Section of part of the vacuolated Golgi region of a Vero cell, 20 hours p.i. Profiles of numerous virus particles, 85–95 nm in diameter, are present within dilated cisternae; some particles (small arrows) show a pedicellar attachment to the cisternal membrane or otherwise indicate a budding process of assembly (small arrow on right). A number of discrete crescent-shaped segments of thickened cisternal membrane are seen in oblique section (large arrows on left). In the *inset* (upper right), a small area of the field is magnified: arrowheads indicate segments, small arrows indicate possible earlier stages of membrane modification. M, mitochondrion. Scale marker: 500 nm. ×37,800; inset, ×59,400.

pear to bud into the lumina of citerna and vacuoles. In addition, profiles of a number of crescent-shaped segments of thickened cisternal membrane are present. The segments are approximately 18 nm in thickness. That such segments, especially those on the lower left of the figure, appear to extend in the direction of the cytoplasmic matrix seems to be due to the oblique plane of section relative to the orientation of the cytomembranes, whose outline is consequently obliterated. In Fig. 3, it may be observed that virus particles possess a limiting trilaminar unit membrane 7–8 nm thick (arrowhead) which is similar to the cellular membranes. The viral membrane seems to possess a very fine fringe about 8 nm deep, of low electron density. The particles are seemingly void of nucleoids or prominent inner shells, despite the fact that the relative thickness of the section might be expected to accentuate such structures if present.

Virions seemed to be exclusively assembled at internal cytomembrane interfaces, and examination of the plasma membrane of infected cells failed to reveal viral budding processes (Figs. 4 and 5). In cells exhibiting marked cytopathic effects, virus release seemed to occur by a mechanism involving dissolution of areas of the plasma and vacuolar membranes with discharge of cell contents and virus, as suggested in Fig. 4. At earlier times after infection, virus release likely occurs by exocytosis, whereby virus particles enclosed either singly or in small groups within membranous enclosures or larger vacuoles are transported to the plasma membrane, where, after membrane fusion

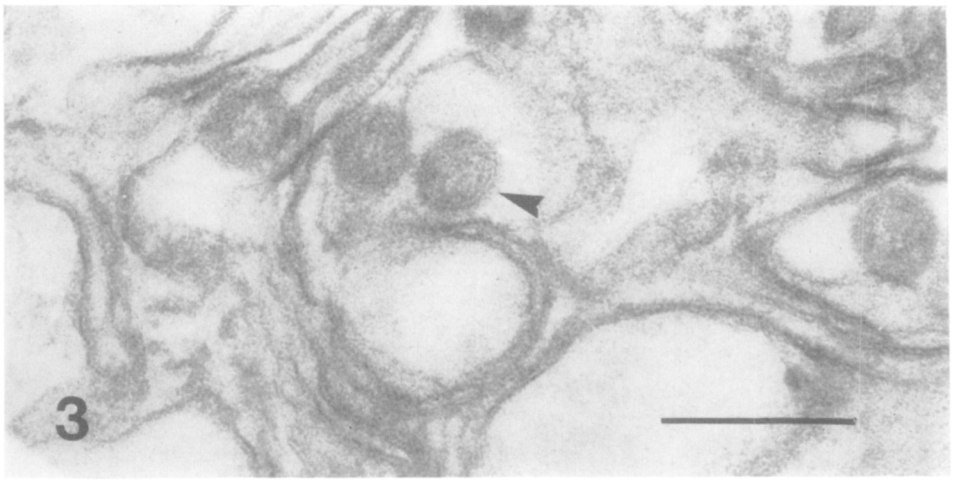

FIG. 3. A typical response to infection in a Vero cell examined 36 hours p.i. is indicated by the proliferation of sheets and tubular elements of smooth endoplasmic reticulum. A number of spherical virus particles are present within cisternae. The virus particle indicated by the arrowhead exhibits a trilaminar limiting membrane with a fine halo, the latter approximately 8 nm thick. Scale marker: 200 nm. ×125,000.

and dissolution of the zone of fused membranes, the virions are released to the exterior of the cell. Such a process is suggested in Fig. 5 (arrow).

Extracellular virions, especially as visualized in specimens taken later after infection e.g., in Fig. 4, appeared to possess ragged, more diffuse, less clearly outlined surfaces than newly elaborated virions within cisternal spaces (Fig. 2). They also appeared to be more uniformly stained.

A preliminary examination of released virions by the negative contrast technique, employing sodium phosphotungstate as the negative stain, was performed on virions, derived from a 48-hr harvest of infectious tissue culture medium, and semipurified by sedimentation on to a 65% sucrose cushion through a 15% sucrose layer. More or less spherical particles, of mean diameter 110 nm, and possessing an outer fringe approximately 12 nm wide were observed. A typical virion is shown (Fig. 5, inset).

Electron Microscopy of Infected A. albopictus Cells

A. albopictus cultures were found to display the three major morphological cell types originally described by Singh (1967) with the small round cell type (6–20 μm in diameter) predominating to the extent of 85–95% of the total. Nuclei were predominantly spherical, occasionally irregular and stellate, and displayed clumps of randomly dispersed chromatin, and nucleoli which were generally unremarkable. The cytoplasmic compartment was generally dense, with extensive granular endoplasmic reticulum, the intracisternal spaces of which were laden with an amorphous product of low density. Microtubules were abundant. Phagocytic vacuoles were a common feature; these contained amorphous globular material and smooth membrane fragments, and in infected cultures frequently showed virus particles at different stages of degradation. Numerous small mitochondria, usually with an open configuration, were commonly observed. Some of the above features are depicted in Fig. 6. Certain cytoplasmic inclusions were a feature of both infected and uninfected cultures, such as aggregates of parallel fibers in paracrystalline array within cisternae of granular endoplasmic reticulum, representing chitin; occasionally septate junctions (Locke, 1965) appeared between cells (unpublished observations).

The low level of virus produced and its rapid release from cells, combined with the fact that only a low percentage of cells were

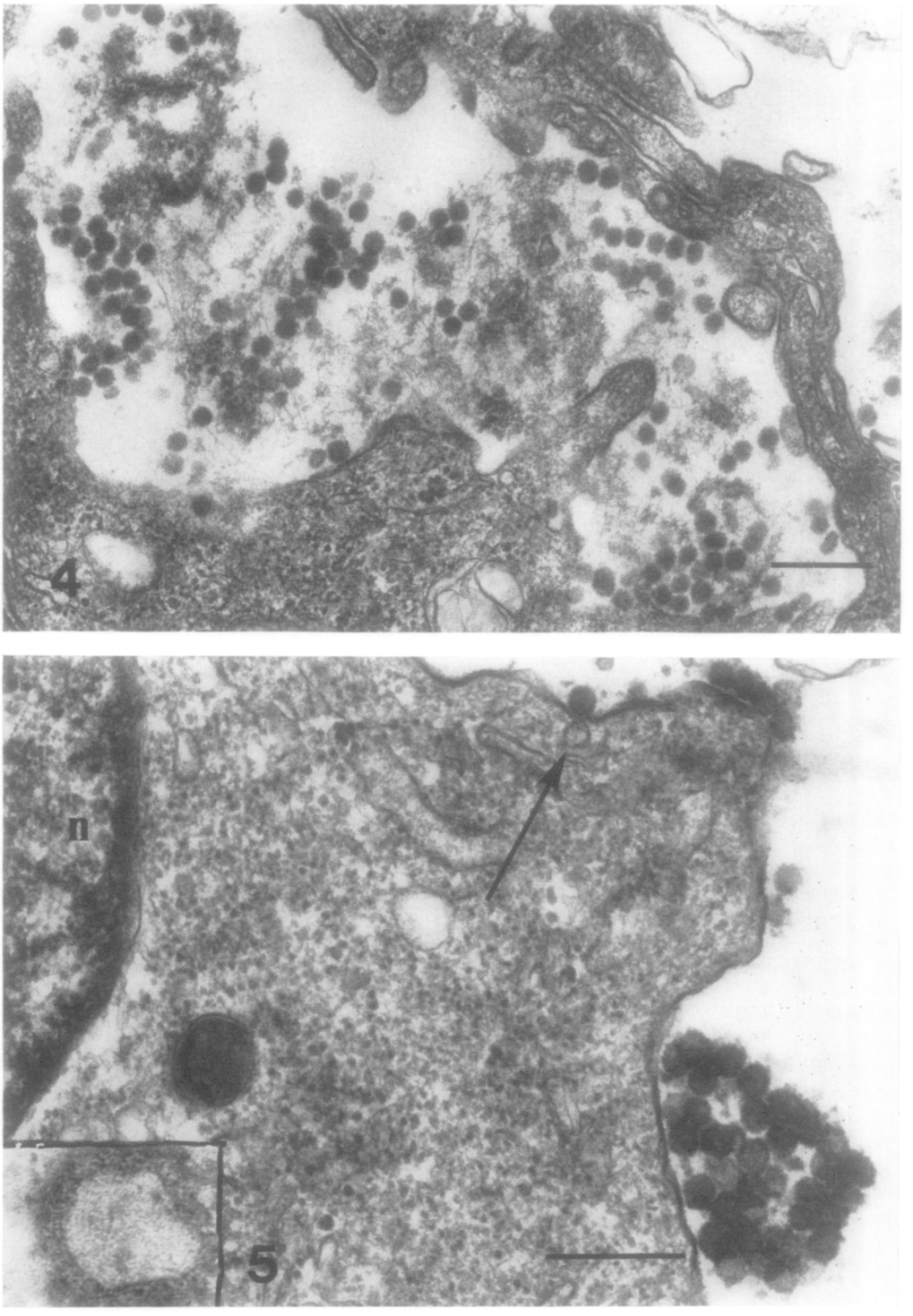

FIG. 4. The portion of the Vero cell (48 hours p.i.) occupying the lower part and sides of the field appears dense through shrinkage. Some focal dissolution of the plasma membrane seems to have occurred, liberating part of cell contents and virus particles into the extracellular space, occupying most of the center of field. Scale marker: 500 nm. ×27,500.

FIG. 5. Section of cytoplasm and nucleus (*n*, on left) of Vero cell 24 hours p.i. Groups of virions lie outisde the plasma membrane on the right of field. The arrow indicates a vesicular membrane which is continuous with the plasma membrane, with a virus particle lying immediately outside the plane of the plasmalemma. Scale marker: 500 nm. ×40,000. *Inset* (lower left): Negative contrast view of a virus particle from a 48-hr harvest of infected Vero cell culture. The ill-defined fringe, composed of fine spicules or loops, is approximately 12 nm deep. ×215,000.

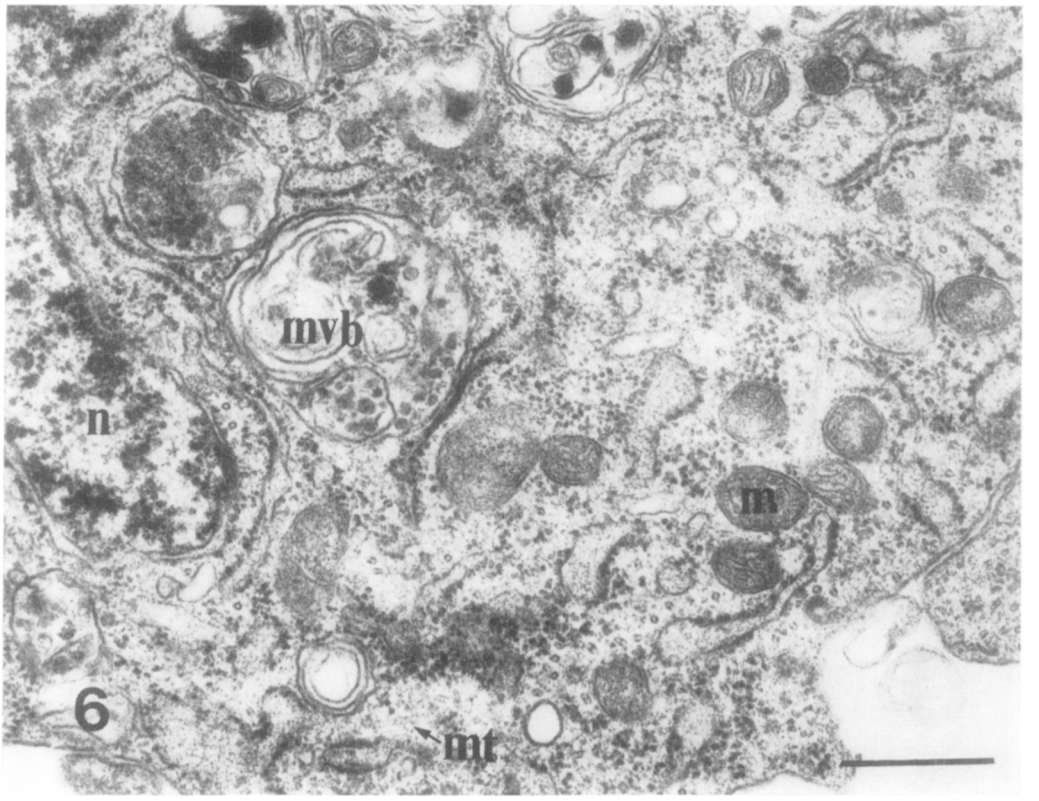

FIG. 6. Portion of the nucleus (*n*) and cytoplasm of typical uninfected *A. albopictus* cell. A number of segments of granular endoplasmic reticulum enclose cisternae which contain a fine granular material. There are numerous free ribosomes within the cytoplasmic matrix as well as numerous microtubules (*mt*), many sectioned transversely and appearing as circles. Profiles of a number of small mitochondria (*m*) are present, and on the left and upper portions of the field there are a number of phagocytic vacuoles and multivesicular bodies (*mvb*) containing smooth membrane fragments and amorphous globular material. Scale marker: 750 nm. ×26,500.

productively infected, made visualization of the features of virus replication difficult. Several hundreds of sections were examined. Nevertheless, at times of maximal virus production, virions were demonstrated within dilated cisternae and vacuoles, and extracellularly. This is shown in Fig. 7. Here, cytopathic effects, in terms of vacuolization and smooth membrane proliferation, are similar to those observed in infected Vero cells. Figure 8 depicts a small section of a degenerating cell, 48 hr post infection, in which a dense layer, 12–14 nm thick, appears to be aligned in close apposition to a short segment of smooth membrane, resembling similar membrane modifications in infected Vero cells (as in Fig. 2). In approximately 7% of infected cells, prominent dense granulofibrillar cytoplasmic masses were found; these were characterized by irregular unstructured margins without limiting membranes (Fig. 9).

In the present experiments the morphological cell type which showed evidence of viral replication was of the predominant small round cell type. What the relative susceptability to infection of the other cell types in the cultures, the spindle-shaped and binucleated cells, could not be ascertained.

Electron Microscopy of Infected Suckling Mouse Brain Cells

Virus-associated cellular changes and evidence of virus replication were rarely seen before 38 hr after infection; at later times cellular changes became progressively more

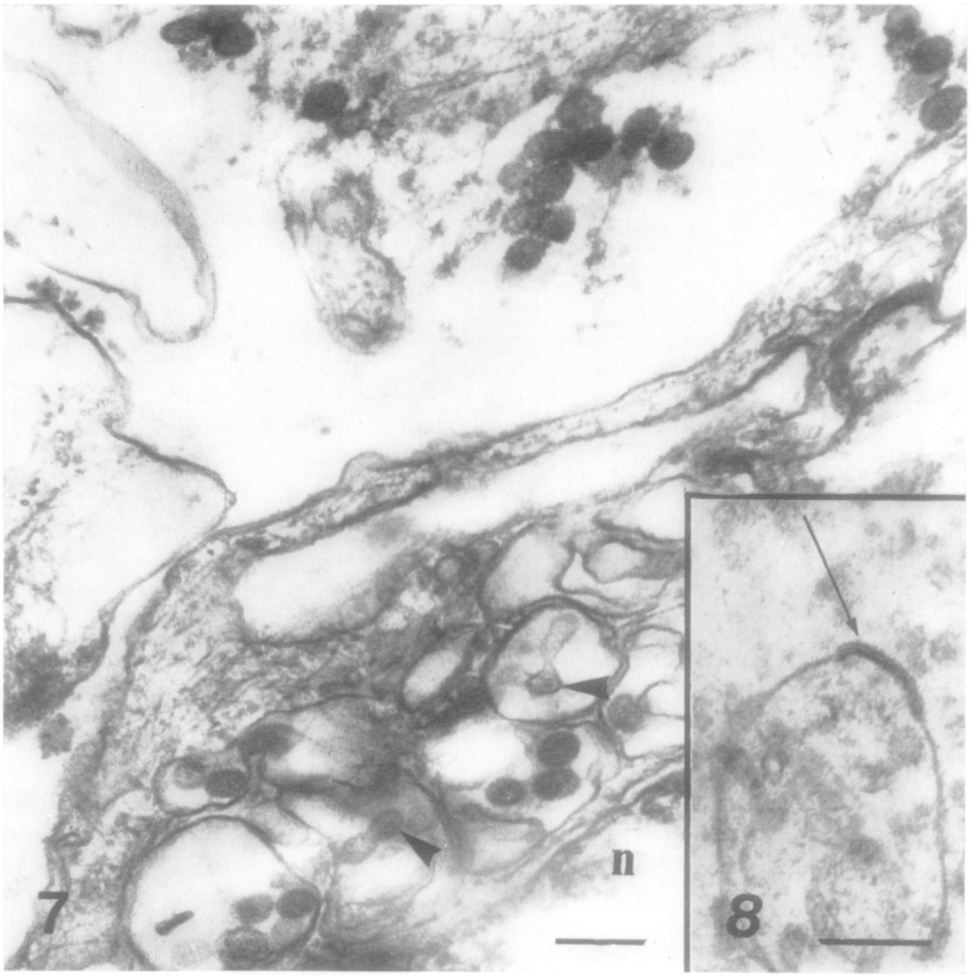

FIG. 7. Part of the vacuolated cytoplasm and the nucleus (*n*) of an *A. albopictus* cell, 24 hrs post infection, occupy the lower part of the field. Typical viral particles are present within vacuoles. Possible viral budding forms are indicated by arrowheads. The viral particles in the upper part of the figure appear to have been shed into an extracellular space. Scale marker: 200 nm. ×50,000.

FIG. 8. A small section of a degenerating mosquito cell, 48 hrs post infection, in which a cytoplasmic process is visualized as extending into a relatively vacuolated space. There is a slight outpouching of a short segment of the cytoplasmic membrane and the alignment underneath, on the cytoplasmic side, of a closely apposed dense layer. Scale marker: 200 nm. ×70,000.

obvious and virus was readily visualized within distended cisternal spaces and vacuoles in the perikaryon of neurons and in dilated extracellular spaces.

An early stage of infection is depicted in Fig. 10, in which the architecture of the tissue appears normal except for the moderately dilated intercellular spaces containing small groups of virions. In the lower small neuron, two vesicle-enclosed virions are arrowed, one of which lies adjacent to the prominent Golgi complex. Examination of a large number of sections at early stages of infection indicated the preeminence of the Golgi apparatus as the site of virus assembly. Figures 11 and 12 are representative. In Fig. 11, the stacked cisternae of the complex are moderately dilated in part; the profile of a virus budding process, in grazing section, is seen extending into the lumen of a cisternal element. Completed virions are seen within cisternae and singly within smooth membranous enclosures. The virus particle on the lower right of the figure

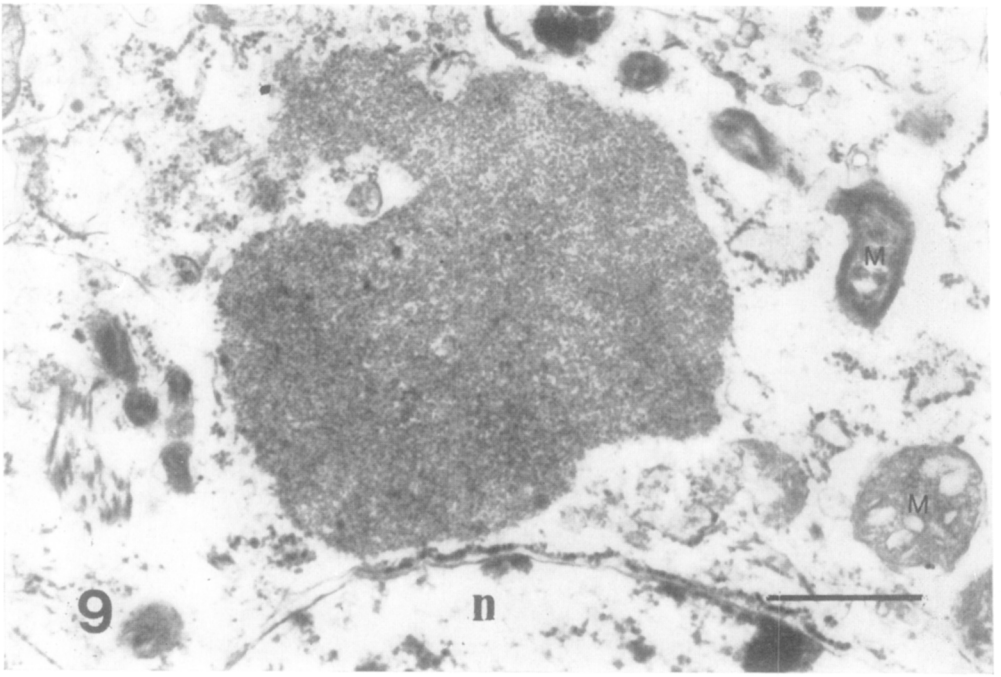

FIG. 9. Section of part of the cytoplasm and nucleus of a mosquito cell, 48 hr post infection, in which a large condensed granulofibrillar inclusion (center of field) is visualized within the cytoplasm. *n*, nucleus; *m*, mitochondria. Scale marker: 500 nm. ×40,000.

(arrowhead) appears to contain a fine inner fibrillar component, 3–5 nm in width. In the inset (Fig. 11, lower left) a viral budding process is depicted in a plane of section which indicates continuity of the limiting membrane of the developing virion with the cisternal membrane. Another example of the involvement of the Golgi complex in viral assembly at early stages of infection is shown in Fig. 12, while at later stages of infection, with increasing cellular vacuolization, viral replication appeared to be topographically more generalized within the cytoplasm (Fig. 13).

Virions located within vacuoles, cisternae, and other membranous enclosures within the cytoplasm of cells (intracellular virions) possessed relatively smooth undifferentiated limiting membranes (e.g., in Fig. 11–13). Virions located in intercellular spaces (extracellular virions), however, appeared to have undergone a modification in their limiting membrane structure insofar as they now exhibited a clearly defined surrounding fringe, about 12 nm in thickness. This is shown in the group of extracellular virions in Fig. 13, inset, lower right.

A fine granulofibrillar matrix adjacent to areas of viral replication, was a common feature of infected brain cells (Figs. 12–15). In such matrices, it was possible to distinguish a fibrillar component, approximately 3 nm in width, which in certain areas appeared wider, 6–7 nm wide, as though assuming a more condensed form (Fig. 15, center arrow). Numbers of small vesiclelike spherical structures, 50–60 nm in diameter, were found enmeshed within such matrices (Figs. 14 and 15). Ribosomes were usually absent.

DISCUSSION

Aspects of virus assembly. Since it was determined that CE virus did not grow to high titers in either of the two-cell culture systems employed in the present study, it became necessary to determine the approximate time at which virus production became maximal. It was reasoned that during this time period, most or all of the morphological features of virus replication would be represented in cells examined by electron microscopy. Inspection of the virus growth curves indicated that cells harvested at times

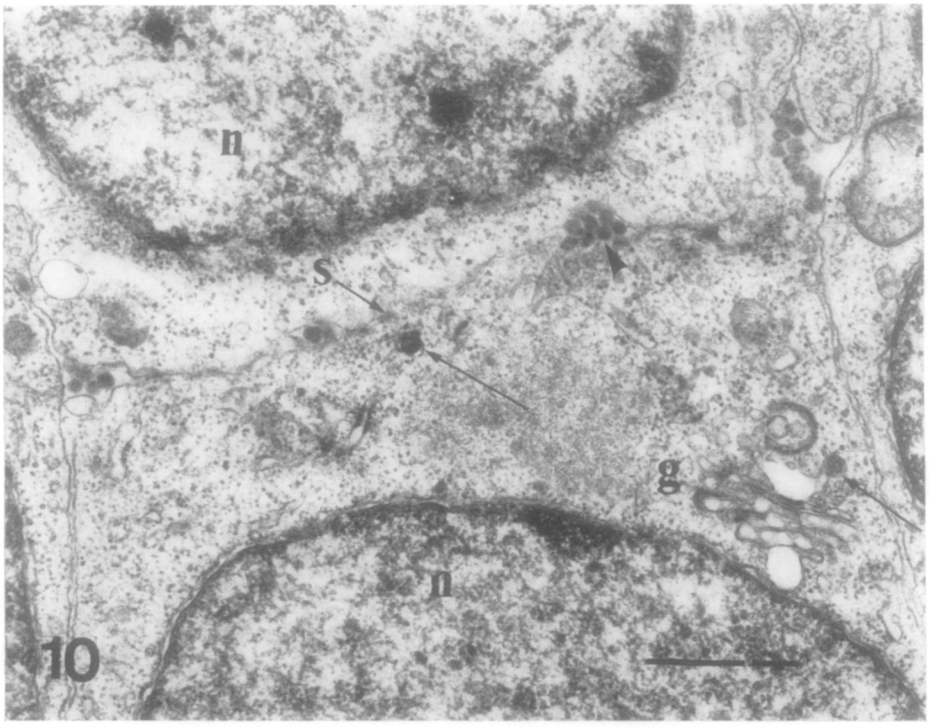

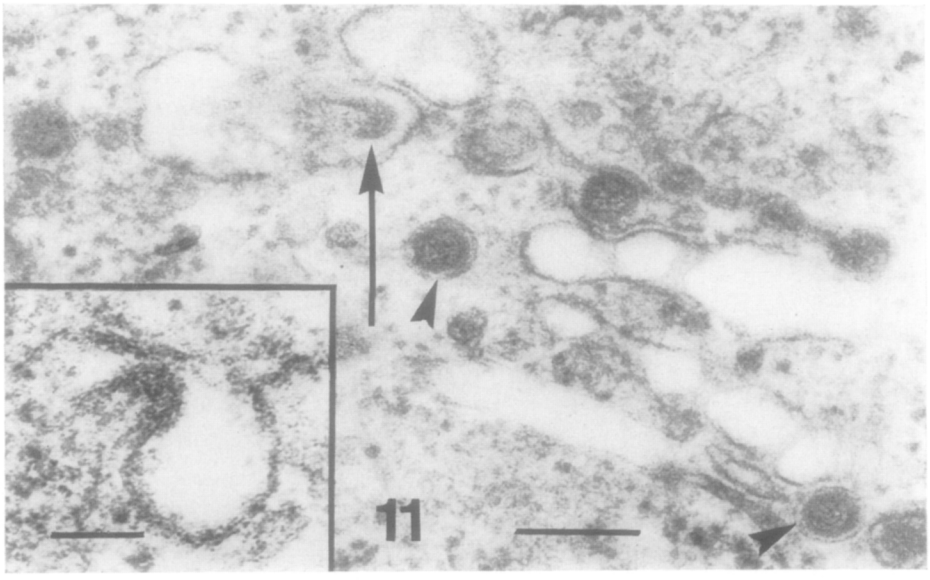

FIG. 10. Section of infected mouse brain, 38 hr post infection showing parts of four small neurons. Single virus particles are present within tight-fitting vesicular membranes (arrows). Groups of virions are present within distended extracellular spaces (arrowhead). There is little cytopathic effect apparent at this stage of infection. *n*, nucleus; *g*, Golgi complex; *s*, synapse at axon terminal. Scaler marker: 1 μm. ×20,000.

FIG. 11. Part of the Golgi region of a neuron, 38 hr after infection. A virus particle, in the process of budding into the lumen of a cisterna is seen in grazing section (arrow). Other virions lie within cisternae and otherwise appear singly within tight-fitting membranous enclosures (arrowheads). The enclosed virion at lower right appears to be pinched off from the end of a cisternal branch. Scale marker: 200 nm. ×80,000. *Inset* (lower left): The virus particle, developing by a budding process into a cisternal space, may be seen to have a trilaminar "unit membrane" which is continuous with and an extension of the cisternal membrane. Scale marker: 100 nm. ×120,000.

later than 16 hr after infection would be valuable in elucidating the course of viral developmental morphology.

In the three cell systems studied, virus assembly was shown to occur exclusively in association with the internal cytomembrane system, thus confirming and extending the original observations of Murphy *et al.*

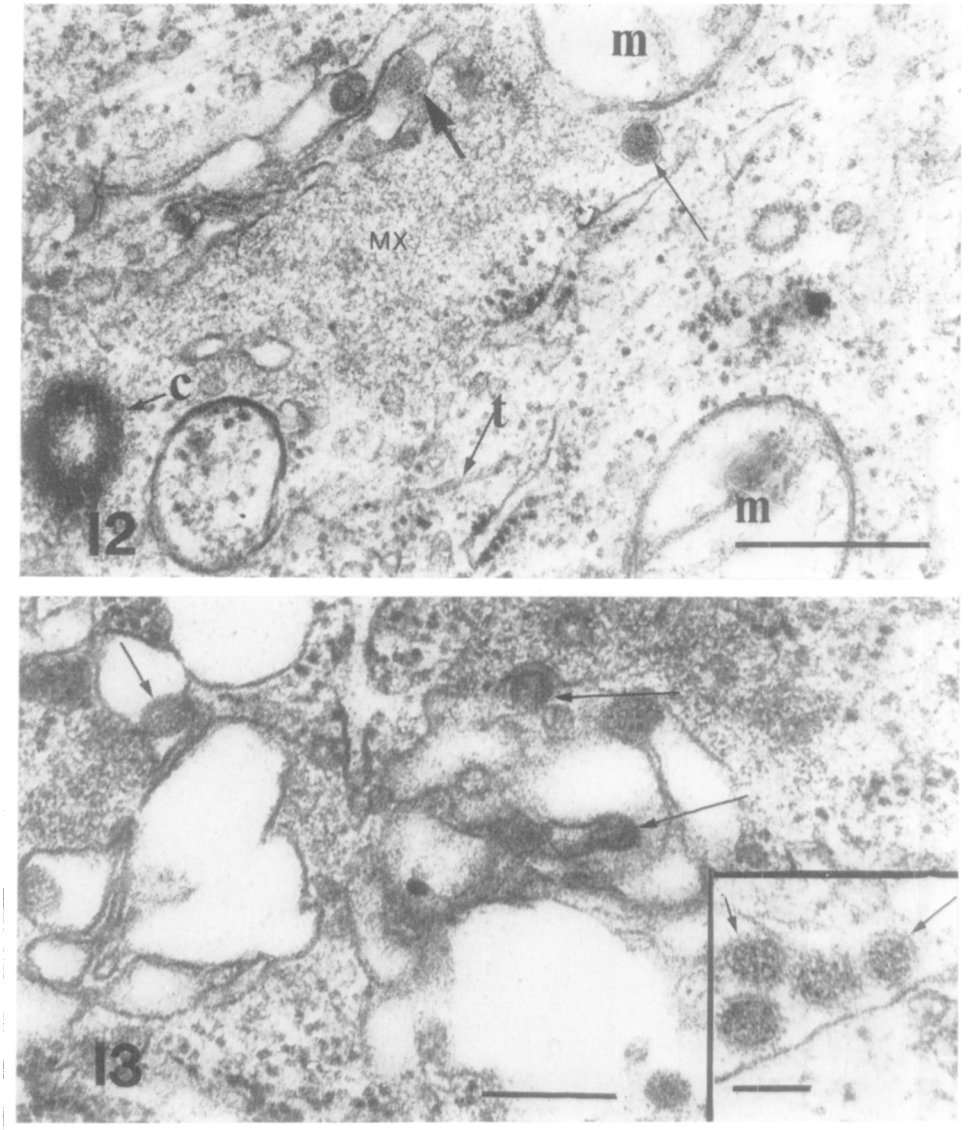

FIG. 12. Part of the cytoplasm of a neuron, 40 hr post infection. A virus particle, developing by budding into the lumen of a Golgi cisterna is depicted (large arrow); a completed virion lies within the cisterna to the left. The slender arrow indicates a virion within a close-fitting membranous enclosure. A fine granulofibrillar matrix (*MX*) lies within the cytoplasm below the Golgi region. A rarely visualized centriole (*c*) is seen on the lower left. *m*, mitochondria; *t*, neurotubule. Scale marker: 500 nm. ×50,000.

FIG. 13. Part of the vacuolated cytoplasm of a neuron at a later stage of infection. Virions are encountered singly (arrow, upper left) or in small groups within vacuoles. Two aspects of viral budding processes are observed (arrows, center of field). Scale marker: 250 nm. ×70,000. *Inset*: A group of mature virions from the same section located extracellularly. These exhibit a well-developed outer fringe 12–14 nm in depth, (arrows) and uniformly electron-dense particle interior. Scale marker: 100 nm. ×100,000.

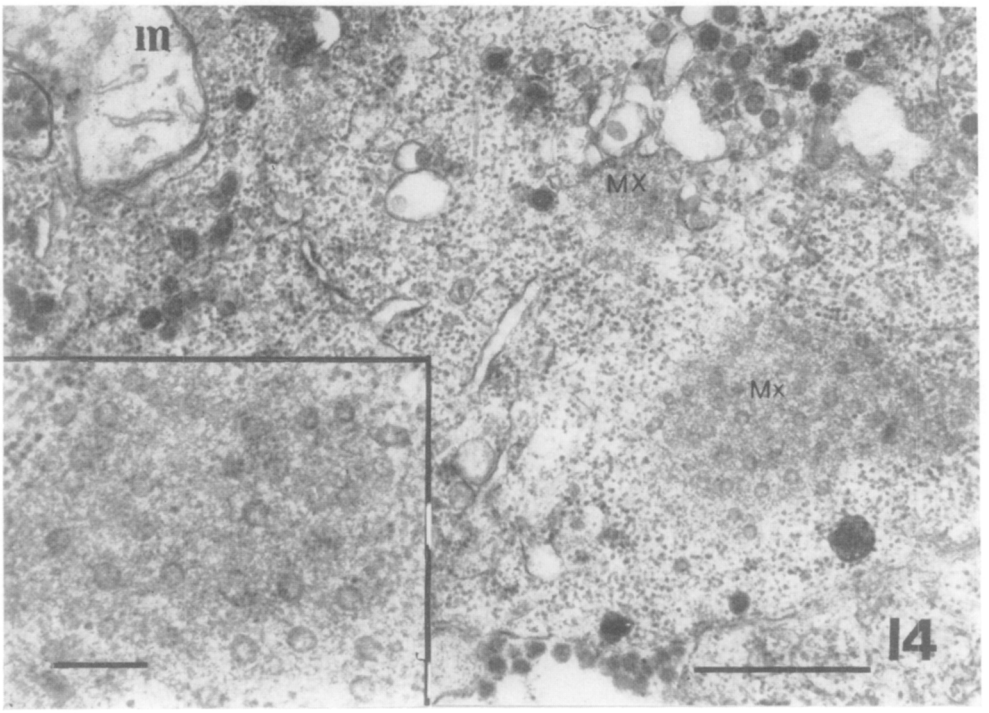

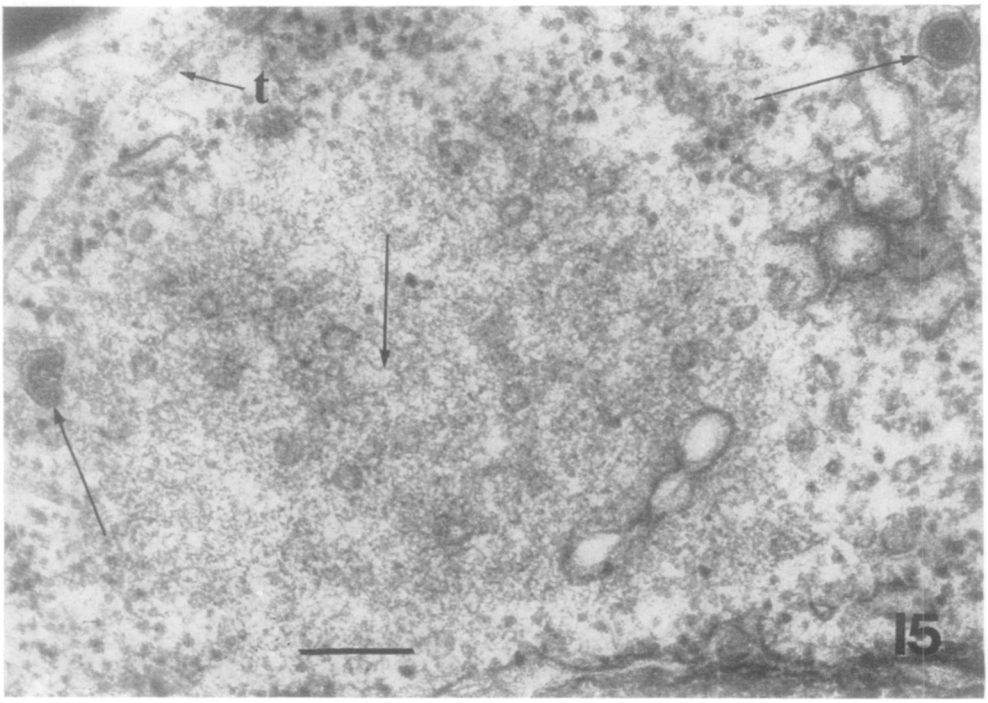

FIG. 14. Part of the cytoplasm of a neuron, 40 hr post infection, showing matrix (*MX*) on right of figure. Numerous 50-60 nm spherical vesicle-like particles are situated within the larger of the masses shown. Numerous cell-associated virus particles are present in characteristic distribution in upper part of field, while a group of extracellular virus particles may be observed in the lower part of the field. *m*, mitochondrion. Scale marker: 1 μm. ×23,000. *Inset*: Part of the matrix with spherical structures. Scale marker: 200 nm. ×60,000.

FIG. 15. Section of part of the cytoplasm of an infected neuron (40 hr p.i.) with part of the nucleus shown on lower right. A granulofibrillar matrix occupies the center of the cytoplasmic field in which fine wavy filamentous structures can be identified (arrow), as well as spherical structures. A completed virion within a membranous enclosure is arrowed on the upper right of field and an incompletely formed virion is arrowed on the left. *t*, neurotubule. Scale marker: 200 nm. ×75,000.

(1968a). The evidence strongly suggested that the Golgi complex represented the initial site of virus replication. Virions appeared to form by budding into the lumina of cisternae and vesicles, acquiring their limiting membrane from the host cell membrane system in the process. A noteworthy finding, in brain cells especially, at early stages of infection, was the presence of virions, individually packaged within close-fitting membranous enclosures. This feature was previously noted by Murphy *et al.* (1968a). The evidence here suggests that these complexes are formed by the segmentation of virus-charged Golgi cisternal elements (Fig. 11). It seems likely that these, as well as larger groups of virions within vacuoles, migrate to the plasma membrane where discharge of the viral particles occurs by the normal discharge process whereby vesicular contents are extruded from cells (Palade and Bruns, 1968). Examination of the plasma membrane of infected cells failed to reveal viral budding processes at this site. Nuclear changes were never observed in infected cells.

The finding in infected Vero cells of discrete segments of thickened cisternal membrane (Fig. 2) provided a possible clue to an early stage of the virus assembly process. It is possible that such structures are formed when viral nucleocapsids align themselves in close apposition to segments of cisternal membrane, modified conceivably, by the insertion of viral-specified proteins. The edges of the membrane segment are visualized as fusing as the budding process is completed at the terminal stage of virus assembly. Altered segments of vesicular membrane were described by Becker *et al.* (1967) in cells infected with avian infections bronchitis virus, a member of the coronavirus group, where they appeared to represent the initial stage of virus assembly. In the present study, stages intermediate between the crescent-shaped membrane complexes and viral buds on pedicellar stalks were not encountered. The envelopment of electron-dense spherical nucleoids, so characteristic a feature of Group A arbovirus assembly (Acheson and Tamm, 1967) has not been observed with California encephalitis virus. Prominent inner shells were not encountered, and only occasionally was there the suggestion of a coiled inner component. The granulofibrillar matrix, in which a relatively uniform-sized population of spherical vesiclelike structures was frequently found, was regularly encountered in areas of the cytoplasm adjacent to sites of virus assembly in brain cells. The matrices appeared to be composed mainly of large aggregates of randomly oriented fine filamentous structures, 3–7 nm in width. Their close topographical relationship to sites of viral assembly, in addition to the fact of their absence in uninfected cells, suggests that they may represent accumulation of viral components such as nucleocapsids and smooth membrane elements, from which milieu virions may sometimes be generated. This is suggested in Fig. 15. Saikku and colleagues (1971) presented evidence suggesting that Inkoo virus, a Finnish subtype of the California encephalitis virus group, possessed a noncubical, filamentous nucleocapsid, the strands of which, in unwound regions measured 2–3 nm in diameter, and in tightly coiled regions measured 7–10 nm. The findings in the present report, while indirect, are not incompatible with those of the Finnish workers. Additional studies with purified CE virus, currently in progress, are clearly necessary to arrive at an unambiguous interpretation of nucleocapsid structure.

Aspects of virus maturation. Cell-associated virions, located within vacuoles and close-fitting membranous enclosures possessed a relatively smooth trilaminar limiting membrane on an exterior aspect of which was a closely adhering fine halo (as seen, for example in Fig. 3). Virions released from cells, on the other hand, appeared to undergo a maturational change in their limiting membrane structure, which became more ragged in appearance, and differentiated to exhibit a fringe of surface projections. This change seems to be accompanied by a redistribution in electron density within the particle; in general, the limiting membrane complex of "intracellular" virions was more densely stained than the interior of the particles, while in extracellular fully mature virions (e.g., in Fig. 13), the well-developed fringe on the exterior of the particles was less densely stained than their interior aspect.

As viewed by the negative contrast technique, this fringe appears to consist of fine spicules or loops, approximately 12 nm in length. The change in surface structure was not as obvious in mosquito cell virions (Fig. 7), although the ragged outline of a number of viral particles (top of figure) suggest a transitional stage.

In the matter of postassembly membrane changes, recent findings of Shapiro and colleagues (1972) are of interest. Working with Japanese encephalitis virus, these workers showed that the viral membrane protein composition changed during morphogenesis; that the intracellular form of the virus contained two glycoproteins while, in extracellular virions one of the glycoproteins appeared to be deglycosylated or replaced by a polypeptide lacking a carbohydrate moiety. It is not known whether such changes were reflected in changes in virus fine structure.

Replication of CE virus in A. albopictus cells. While a few arboviruses have been visualized by electron microscopy in tissue specimens from intact arthropods (e.g., Bergold and Weibel, 1962; Bowne and Jones 1966), similar studies have not been reported for cultures arthropod cells, with the exception of the study by Filshie and Rehacek (1968) of the growth of two group B arboviruses, Japanese encephalitis and Murray Valley encephalitis viruses in a line of *A. aegypti* cells.

In the present study it was interesting to note that the *A. albopictus* cells, despite a culture history of almost 300 serial passages, still tended to express differentiated functions, as indicated by chitin synthesis and the formation of specialized septate junctions (unpublished observations). It would appear that they constitute a useful model system for providing insights into the problems of virus–cell interactions in the intact mosquito.

The virus particles were similar in size, general morphology and cellular distribution to those observed in Vero cells and brain. The dense granulofibrillar inclusions encountered in a low percentage of infected mosquito cells show some resemblances to inclusions found in Vero cells infected with certain members of the arenavirus group (Murphy *et al.*, 1970).

At the light microscopic level of inspection, no cytopathic effects of any consequence were demonstrable in the infected mosquito cell cultures. The growth rate of cells from persistently infected and noninfected cultures was comparable (unpublished observation). The infectious center assay reported here indicated that a low proportion of cells was productively infected. The results of the electron microscopic study, although meager, indicated that for a certain proportion of cells at least, infection with California encephalitis virus was lethal. It is likely that such lethally infected cells were replaced with a sufficient number of sensitive cells to establish a steady-state interaction, partially explaining, at least, the phenomenon of viral persistence in the *A. albopictus* cultures. Other possible parameters, defining this carrier state, have not yet been elucidated.

ACKNOWLEDGEMENTS

This investigation was supported by Public Health Service research grant A109182 from the National Institute of Allergy and Infectious Diseases, and by a grant from the Lillia Babbitt Hyde Foundation.

REFERENCES

Acheson, N. H., and Tamm, I. (1967). Replication of Semliki Forest virus: an electron microscopic study. *Virology* **32**, 128–143.

Becker, W. B., McIntosh, K., Dees, J. H., and Chanock, R. M., (1967). Morphogenesis of avian infectious bronchitis virus and a related human virus (Strain 229E). *J. Virol.* **1**, 1019–1027.

Bergold, G. H., and Weibel, J. (1962). Demonstration of yellow fever virus with the electron microscope. *Virology* **17**, 554–562.

Bowne, J. G., and Jones, R. H. (1966). Observations on bluetongue virus in the salivary glands of an insect vector. *Culicoides vari-ipennis. Virology* **30**, 127–133.

Came, P. E., Pascale, A., and Shimonaski, G., (1968). Effect of pancreatin on plaque formation by influenza viruses. *Arch. Gesamte Virusforsch.* **23**, 346–352.

Filshie, B. K., and Rehacek, J., (1968). Studies of the morphology of Murray Valley encephalitis and Japanese encephalitis viruses growing in cultured mosquito cells. *Virology* **34**, 435–443.

HOLMES, I. H. (1971). Morphological similarity of Bunyamwera supergroup viruses. *Virology* **43**, 708–712.

LOCKE, M. (1965). The structure of septate desmosomes. *J. Cell Biol.* **25**, 166–169.

MURPHY, F. A., WHITFIELD, S. G., COLEMAN, P. H., CALISHER, C. H., RABIN, E. R., JENSON, A. B., MELNICK, J. L., EDWARDS, M. R., AND WHITNEY, E., (1968a). California group arboviruses: electron microscopic studies. *Exp. Mol. Pathol.* **9**, 44–56.

MURPHY, F. A., HARRISON, A. K., AND TZIANABOS, T. (1968b). Electron microscopic observations of mouse brain infected with Bunyamwera group arboviruses. *J. Virol.* **2**, 1315–1325.

MURPHY, F. A., WEBB, P. A., JOHNSON, K. M., WHITFIELD, S. G., AND CHAPPEL, W. A. (1970). Arenoviruses in Vero cells: Ultrastructural studies. *Virology* **6**, 507–518.

PALADE, G. E., AND BRUNS, R. R. (1968). Structural modulations of plasmalemmal vesicles. *J. Cell Biol.* **37**, 633–649.

SAIKKU, P., VON BONSDORFF, C. H., BRUMMER-KORVENKONTIO, M., AND VAHERI, A. (1971). Isolation of non-cubical ribonucleoprotein from Inkoo virus, a Bunyamwera supergroup arbovirus. *J. Gen. Virol.* **13**, 335–337.

SHAPIRO, D., BRANDT, W. E., AND RUSSELL, P. K. (1972). Change involving a viral membrane glycoprotein during morphogenesis of a Group B arbovirus. *Virology* **50**, 906, 911.

SINGH, K. R. P. (1967). Cell cultures derived from larvae of *Aedes albopictus* (skuse) and *A. aegypti* (L). *Curr. Sci.* **36**, 506–508.

STIM, T. B., AND HENDERSON, J. R. (1969). Arbovirus plaquing in a clonal line (PS Y-15) of porcine kidney. *Appl. Microbiol.* **17**, 246–249.